One-step Nucleic Acid Amplification for Intraoperative Detection of Lymph Node Metastasis in Breast Cancer Patients

Masahiko Tsujimoto,[1] Kadzuki Nakabayashi,[14] Katsuhide Yoshidome,[2] Tomoyo Kaneko,[8] Takuji Iwase,[9] Futoshi Akiyama,[8] Yo Kato,[8] Hitoshi Tsuda,[12] Shigeto Ueda,[13] Kazuhiko Sato,[13] Yasuhiro Tamaki,[3] Shinzaburo Noguchi,[3] Tatsuki R. Kataoka,[4] Hiromu Nakajima,[5] Yoshifumi Komoike,[6] Hideo Inaji,[6] Koichiro Tsugawa,[11] Koyu Suzuki,[10] Seigo Nakamura,[11] Motonari Daitoh,[14] Yasuhiro Otomo,[14] and Nariaki Matsuura[7]

Abstract

Purpose: Detection of sentinel lymph node (SLN) metastasis in breast cancer patients has conventionally been determined by intraoperative histopathologic examination of frozen sections followed by definitive postoperative examination of permanent sections. The purpose of this study is to develop a more efficient method for intraoperative detection of lymph node metastasis.

Experimental Design: Cutoff values to distinguish macrometastasis, micrometastasis, and nonmetastasis were determined by measuring cytokeratin 19 (CK19) mRNA in histopathologically positive and negative lymph nodes using one-step nucleic acid amplification (OSNA). In an intraoperative clinical study involving six facilities, 325 lymph nodes (101 patients), including 81 SLNs, were divided into four blocks. Alternate blocks were used for the OSNA assay with CK19 mRNA, and the remaining blocks were used for H&E and CK19 immunohistochemistry–based three-level histopathologic examination. The results from the two methods were then compared.

Results: We established CK19 mRNA cutoff values of 2.5×10^2 and 5×10^3 copies/μL. In the clinical study, an overall concordance rate between the OSNA assay and the three-level histopathology was 98.2%. Similar results were obtained with 81 SLNs. The OSNA assay discriminated macrometastasis from micrometastasis. No false positive was observed in the OSNA assay of 144 histopathologically negative lymph nodes from pN0 patients, indicating an extremely low false positive for the OSNA assay.

Conclusion: The OSNA assay of half of a lymph node provided results similar to those of three-level histopathology. Clinical results indicate that the OSNA assay provides a useful intraoperative detection method of lymph node metastasis in breast cancer patients.

Sentinel lymph node (SLN) biopsy has recently become a standard surgical procedure in the treatment of breast cancer patients (1–10). This procedure can predict metastasis to the regional lymph nodes with high accuracy and avoids unnecessary removal of axillary lymph nodes and subsequent morbidity associated with axially clearance in node negative breast cancer patients.

SLN metastasis is generally detected by conventional means including the intraoperative H&E-based histopathologic examination of frozen section(s) or cytologic observation of touch-imprints, followed by definitive postoperative histopathologic examination of permanent sections (2, 7–9). However, the sensitivity of these intraoperative methods is not high. Many investigators have reported that the intraoperative H&E-based histopathologic examination has a false-negative rate of 5% to 52% (reviewed in ref. 11). Furthermore, these methods provide subjective rather than objective results, which may differ from one pathologist to another (12). On the other hand, the definitive postoperative histopathologic examination generally requires 5 to 10 days for assessment. If an accurate

Authors' Affiliations: Departments of [1]Pathology and [2]Surgery, Osaka Police Hospital, [3]Department of Breast and Endocrine Surgery, Osaka University Graduate School of Medicine, Departments of [4]Pathology, [5]Clinical Laboratory, and [6]Surgery, Osaka Medical Center for Cancer and Cardiovascular Diseases, and [7]Department of Molecular Pathology, Osaka University Graduate School of Medicine and Health Science, Osaka, Japan; Departments of [8]Pathology and [9]Breast Surgery, Cancer Institute of the Japanese Foundation for Cancer Research, and Departments of [10]Pathology and [11]Breast Surgical Oncology, St. Luke's International Hospital, Tokyo, Japan; Departments of [12]Pathology II and [13]Surgery I, National Defense Medical College, Saitama, Japan; and [14]Central Research Laboratories, Sysmex Corp., Kobe, Japan

Received 10/16/06; revised 4/3/07; accepted 5/15/07.

The costs of publication of this article were defrayed in part by the payment of page charges. This article must therefore be hereby marked *advertisement* in accordance with 18 U.S.C. Section 1734 solely to indicate this fact.

Note: Supplementary data for this article are available at Clinical Cancer Research Online (http://clincancerres.aacrjournals.org/).

M. Tsujimoto and K. Nakabayashi contributed equally to this work.

Requests for reprints: Nariaki Matsuura, Department of Molecular Pathology, Graduate School of Medicine and Health Science, Osaka University, 1-7 Yamadaoka, Suita, Osaka 565-0817, Japan. E-mail: matsuura@sahs.med.osaka-u.ac.jp.

doi:10.1158/1078-0432.CCR-06-2512

intraoperative method is developed, the test results can allow for completion of axillary node dissection during surgery and avoidance of a second surgical procedure in patients with positive SLNs, thereby reducing patient distress and, finally, saving hospital costs (2, 13, 14). Accordingly, the development of a precise and objective intraoperative method for the detection of lymph node metastasis is important for increasing the efficiency of breast cancer surgery (10, 13–18).

To overcome the shortcomings of the present histopathologic methods, molecular biological methods based on quantitative reverse transcription-PCR (QRT-PCR) have been studied extensively for the detection of lymph node metastasis in breast cancer patients (12, 19–25). A QRT-PCR assay with multiple mRNA markers including cytokeratin 19 (CK19), trefoil factor 3 (p1B), epithelial glycoprotein 2 (EGP2), and small breast epithelial mucin (SBEM) resulted in a 10% upstaging compared with the routine histopathologic analysis (22). It was also reported that a QRT-PCR assay using mRNA markers of CK19 and mammaglobin 1 (MGB1) was almost as accurate (94.1% sensitivity and 98.6% specificity) as that of the conventional histopathologic examination (12). This study included a discussion of the drawbacks of using a single marker like CK19 mRNA for which the QRT-PCR may include the concomitant amplification of CK19 pseudogenes within genomic DNA, giving false positive results.

We recently developed a one-step nucleic acid amplification (OSNA) assay (Fig. 1A), which consists of solubilization of a lymph node followed by reverse-transcription loop-mediated isothermal amplification (RT-LAMP) of a target mRNA (26, 27). The RT-LAMP reaction is a new method of gene amplification, and its application has been reported previously (28–32). The OSNA method is characterized by the quantitative measurement of a target mRNA in a metastatic lymph node, a brief reaction time for the OSNA process, a high specificity for the target mRNA, and an absence of genomic DNA amplification.

In this paper, we report an efficient intraoperative detection method for lymph node metastasis in breast cancer patients using the OSNA assay with CK19 mRNA as a target marker. The results of a multicenter clinical study including 325 lymph nodes are discussed from the viewpoint of the usefulness of the OSNA assay as an intraoperative detection method.

Materials and Methods

Lymph nodes for selection of mRNA markers and determination of cutoff values. Lymph nodes, which were used to select mRNA markers and determine cutoff values, were obtained from Osaka Police Hospital with the approval of its internal review board. Lymph nodes were stored at -80°C until use.

QRT-PCR. QRT-PCR was carried out by ABI Prism 7700 sequence detector. RNA was purified from a lymph node lysate using RNeasy Mini Kit (Qiagen), and then purified RNA was subjected to one-step RT-PCR with QuantiTect SYBR Green (Qiagen) according to the manufacturer's instructions. The sequences of the forward and reverse primers used are shown in Supplementary Table S1. The primers were designed by Primer Express Version 2.0 software (ABI).

Selection of mRNA maker. Forty-five candidate mRNA markers, selected as being specific to breast cancer tissue, were identified from the public EST database (33). The performance of these mRNA markers was evaluated with QRT-PCR using a mixture of four histopathologically positive and four negative lymph nodes. The results were summarized as C_t (threshold cycle) values for each mRNA marker (see Supplementary Table S2). The selected markers, KRT19 (CK19), CEACAM5 (CEA), forkhead box A1 (FOXA1), SAM-pointed domain containing ETS transcription factor (SPDEF), tumor-associated calcium signal transducer 2 (TACSTD-2), mucin 1 (MUC1), and MGB1, were further evaluated with QRT-PCR using 11 histopathologically positive and 15 negative lymph nodes from 26 patients.

RT-LAMP reaction of CK19 mRNA. The RT-LAMP reaction was carried out according to the Notomi's method (26, 27). The human CK19 mRNA was synthesized by *in vitro* transcription from cloned cDNA.

A 2-μL sample of human CK19 mRNA in a lysis buffer containing 200 mmol/L glycine-HCl, 20% DMSO, and 5% Brij35 (pH 3.5) was added to 23 μL of solution consisting of 3.5 μmol/L each of the forward inner (CK19FA) and reverse primer (CK19RA), 0.2 μmol/L each of forward outer (CK19F3) and reverse primer (CK19R3), 2.6 μmol/L each of forward loop (CK19LPF) and reverse primer (CK19LPR), 0.9 mmol/L deoxynucleotide triphosphates, 54.3 mmol/L Tris-HCl, 10.8 mmol/L KCl, 10.8 mmol/L $(NH_4)_2SO_4$, 5.4 mmol/L $MgSO_4$, 0.1% Triton X-100, 5.4 mmol/L DTT, 2.5 units avian myeloblastosis virus reverse transcriptase (Promega), 18 units Bst DNA Polymerase (New England Biolabs), and 25 units RNasin Plus (Promega). Each reaction mixture contained three pairs of primer sets including the loop primer (27). The sequences of the human CK19 primers were designed as amplicons spanning exon junction regions between CK19 exons 1 and 2 and were

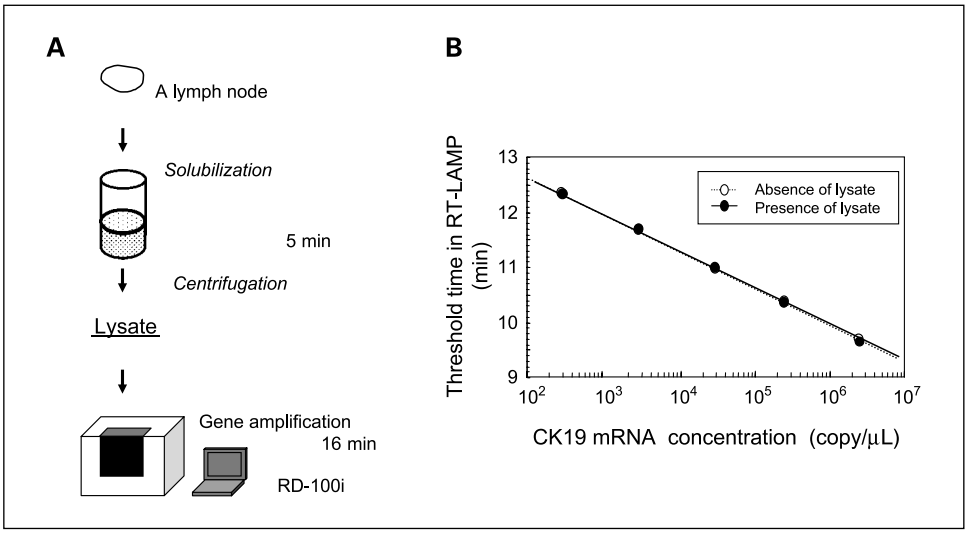

Fig. 1. OSNA assay. *A,* schematic diagram of the OSNA procedure. *B,* standard curve of human CK19 mRNA measured by RD-100i in the presence and absence of lymph node lysate. A histopathologically negative lymph node (600 mg) was homogenized in 4 mL of lysis buffer. A 180-μL sample of the lymph node lysate was added to 20 μL of human CK19 mRNA in the lysis buffer. The final concentration of human CK19 mRNA was adjusted to 2.5×10^6, 2.5×10^5, 2.5×10^4, 2.5×10^3, and 2.5×10^2 copies/μL. A 2-μL sample of each was subjected to the RT-LAMP reaction under the same conditions described in Materials and Methods.

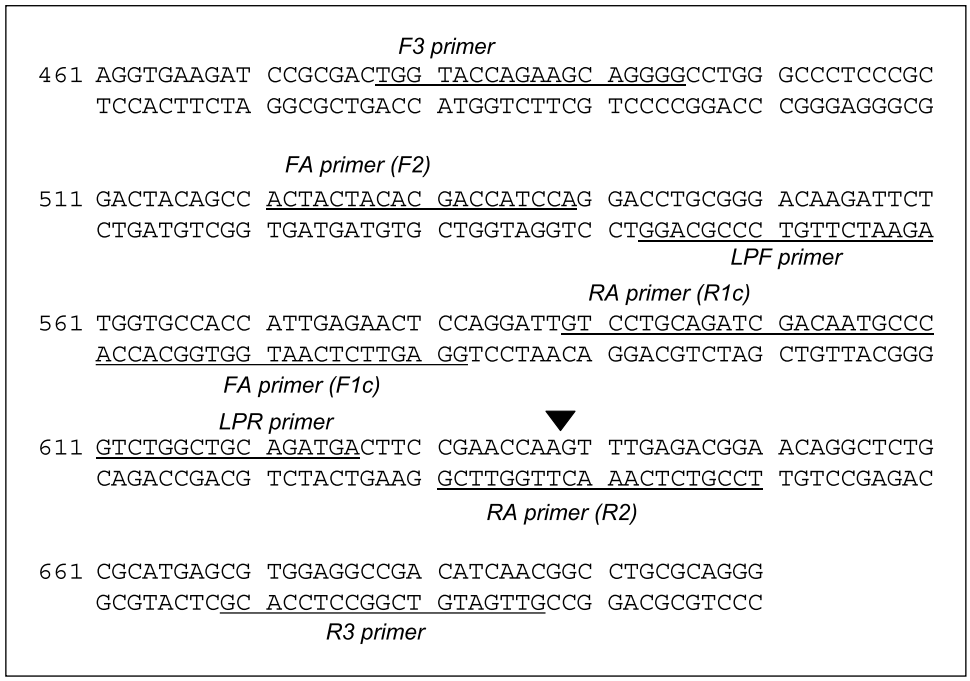

Fig. 2. A schematic representation of primer placement along the CK19 cDNA sequence. The CK19 cDNA sequence (NM.002276) and the sequence of the primers for the CK19 RT-LAMP are shown. The location on CK19 cDNA where each primer-set binds is underlined. The sequence of the inner primer (FA and RA) consists of discontinuous two different regions, F1c and F2 (or R1c and R2), to create the stem structure during the RT-LAMP reaction. The exon junction between exons 2 and 3 is included in the sequence of the R2 region in the RA primer (*arrowhead*).

furthermore designed as mismatch sequences of the CK19a and CK19b pseudogenes (GenBank accession number M33101 and U85961) using Probe Wizard (RNAture). Primer sequences were 5′-GGAGTTCT-CAATGGTGGCACCAACTACTACACGACCATCCA-3′ (CK19FA), 5′-GTCCTGCAGATCGACAACGCCTCCGTCTCAAACTTGGTTCG-3′ (CK19RA), 5′-TGGTACCAGAAGCAGGGG-3′ (CK19F3), 5′-GTTGATGTCGGCCTCCACG-3′ (CK19R3), 5′-AGAATCTTGTCCCG-CAGG-3′ (CK19LPF), and 5′-CGTCTGGCTGCAGATGA-3′ (CK19LPR). The sequence of each primer and its placement along the CK19 cDNA sequence are shown in Fig. 2.

The RT-LAMP reaction with CK19 mRNA was carried out in a gene amplification detector, RD-100i (Sysmex). Mori et al. (34, 35) reported that PPi, which is produced in the course of the RT-LAMP reaction, binds to magnesium ion to result in magnesium PPi. The amount of magnesium PPi increases with the passage of the reaction. Magnesium PPi has a low solubility in aqueous solution and precipitates when its concentration reaches saturation. The amplification of CK19 mRNA was monitored by measuring the turbidity of the reaction mixture at 6-s intervals. The threshold time was defined as the time at which the turbidity exceeded 0.1.

OSNA assay. A schematic diagram of the OSNA assay with CK19 mRNA is shown in Fig. 1A. A histopathologically negative lymph node (≤600 mg) was homogenized in 4 mL of the above lysis buffer for 90 s on ice using a Physicotron Warring blender with an NS-4 shaft (MicroTec Nichion). The homogenate was centrifuged at 10,000 × *g* for 1 min at room temperature. A 2-μL sample of the supernatant (lysate) was subjected to the RT-LAMP reaction under the same conditions as above. CK19 mRNA copy number was determined based on the standard curve using a known quantity of human CK19 mRNA.

Effect of lymph node size on the OSNA assay. A histopathologically negative lymph node (130 mg) was homogenized in 4 mL of lysis buffer under the same conditions as above. A 180-μL sample of lymph node lysate was added to 20 μL of human CK19 mRNA in the lysis buffer. The final concentration of human CK19 mRNA was adjusted to 2.5×10^5 and 2.5×10^3 copies/μL. About 2 μL of each sample was subjected to the RT-LAMP reaction under the same conditions described above. Each sample was assayed in duplicate. Other histopathologically negative lymph nodes (214, 354, and 428 mg) were treated under the same conditions as above.

Amplification of genomic DNA by the OSNA assay. Genomic DNA was extracted from histopathologically positive lymph nodes using QIAamp DNA Mini Kit (Qiagen) according to the manufacturer's instructions. Purified genomic DNA (100 ng) was subjected to the OSNA assay using the CK19 primers described above.

Protocol for determining the cutoff values. A cutoff value (L) for the OSNA assay between metastatic positive and negative lymph nodes was determined using 106 lymph nodes (42 histopathologically negative lymph nodes from pN0 patients, 42 histopathologically negative lymph nodes from pN1-3 patients, and 22 histopathologically positive lymph nodes) from 30 patients (24 ductal carcinomas, 5 special types, and 1 ductal carcinoma *in situ*). As shown in Fig. 3A, the central part of one quarter of a frozen lymph node (40-600 mg) of 1 mm thickness was dissected out. Four levels (i, ii, iii, and iv) were used as permanent slices for the histopathologic examination with H&E and immunohistochemistry using anti-CK19 antibody (DAKO) as shown in Fig. 3A.

Histopathologically positive lymph nodes were defined as those that were positive at any of four levels (i, ii, iii, and iv). Histopathologically negative lymph nodes were defined as those that were negative in all four levels. Blocks a and c were used for the OSNA assay. A cutoff value was determined by statistical analysis of the copy numbers obtained by the OSNA assay of the histopathologically negative lymph nodes from pN0 patients.

According to the tumor-node-metastasis (TNM) classification of the Unio Internationale Contra Cancrum (Italian) sixth and the American Joint Committee on Cancer sixth editions (36), macrometastasis is defined as having metastatic foci of ≥2 mm in the long axis. In the OSNA assay, macrometastasis is assumed as having the amount of CK19 mRNA expression in 2^3 mm^3 of metastatic foci. Based on this assumption, we estimated a cutoff value (H) for CK19 mRNA between macrometastasis and micrometastasis as follows. Nine frozen histopathologically positive lymph nodes from nine breast cancer patients (8 ductal and 1 lobular carcinomas) were used to estimate the amount of CK19 mRNA expression in 2^3 mm^3 of metastatic foci (Table 1). A frozen lymph node was serially sectioned at 10-μm intervals. Each slice was first examined with CK19 immunohistochemistry–based histopathologic examination to measure the area of metastatic foci and then with RT-LAMP to measure CK19 mRNA expression. The procedure is detailed in Fig. 3B.

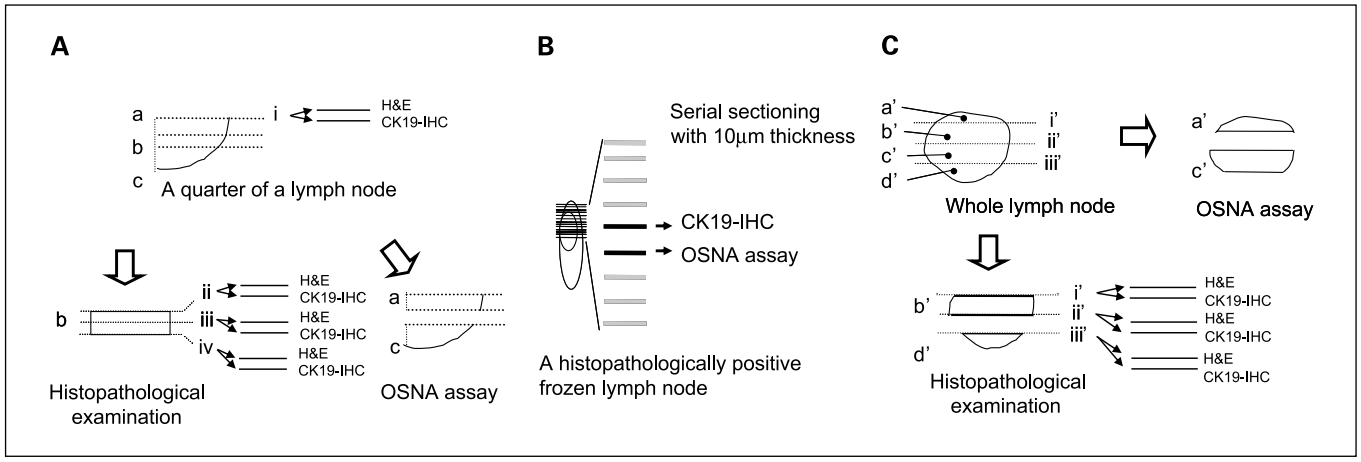

Fig. 3. Protocols. *A,* protocol for determining a cutoff value for micrometastasis and nonmetastasis. *B,* protocol for determining the cutoff value between macrometastasis and micrometastasis. Serial frozen sections taken at 10-μm intervals were prepared from histopathologically positive lymph nodes. One of two consecutive frozen sections was subjected to CK19 immunohistochemistry (CK19-IHC) – based histopathologic examination to measure the area of metastatic foci, and then the volume of the metastatic foci was calculated by multiplying the area by the thickness of the slice. The adjacent section was subjected to the OSNA assay. The expression level of CK19 mRNA in 2^3 mm^3 was estimated based on the correlation between the volume of metastatic foci and CK19 mRNA expression. *C,* clinical study protocol.

In the OSNA assay, an amount of CK19 mRNA expression less than the cutoff value was indicated as (-), an amount of CK19 mRNA expression between the cutoff values *L* and *H* was indicated as (+), and an amount of CK19 mRNA expression greater than the cutoff value *H* was indicated as (++).

Clinical study protocol. An intraoperative clinical study was conducted from February 2005 to July 2005 at six facilities other than Sysmex Central Research Laboratories. A total of 325 fresh lymph nodes (101 patients), including 81 SLNs (49 patients), were used with the approval of the internal review board at each facility. The clinicopathologic characteristics of patients are shown in Table 2. A large percent of patients had stages I A/B and II A/B. The majority of patients had a nodal status of pN0 and pN1. About 80% of patients had invasive ductal carcinoma.

A fresh lymph node with a short axis of 4 to 12 mm was divided into four blocks at 1- or 2-mm intervals using our original cutting device (Fig. 3C and 4). Blocks a′ and c′ were used for the OSNA assay. Two slices were cut from each of the three cutting surfaces (i′, ii′, and iii′), as shown in Fig. 3C, and used for the permanent three-level histopathologic examination with H&E and CK19 immunohistochemistry.

In the histopathologic examination, macrometastasis and micrometastasis were defined according to the TNM classification of the Unio Internationale Contra Cancrum sixth and American Joint Committee on Cancer sixth editions (36). All samples for histopathologic examination were examined by three third-party pathologists. Conflicting results were settled consensually. The performance of the OSNA assay was compared with the three-level histopathology.

The OSNA assay analyzed different blocks from those used in the three-level histopathologic examination. Therefore, in this protocol, the sensitivity and specificity of the OSNA assay could not be calculated based on the histopathologic results. For this reason, we evaluated the performance of the OSNA assay as a concordance rate with the three-level histopathologic examination.

In the case of lymph nodes from pN0 patients, blocks b′ and d′ were further sliced at 0.2-mm intervals, followed by staining each alternate slice with H&E and CK19 immunohistochemistry (Fig. 3C). A total of 144 lymph nodes, in which neither macrometastasis nor micrometastasis were observed in the above serial sectioning examination, were used for the false positive study of the OSNA assay.

When discordance between the OSNA assay and the three-level histopathologic examination occurred, a histopathologic analysis of blocks b′ and d′ was repeated. All slides for the histopathologic examination were examined and evaluated by three third-party pathologists. All results of histopathologic examinations were finally determined by a study group comprised of representatives from the different facilities.

Analysis of discordant cases. In the analysis of discordant cases, QRT-PCR and CK19 Western blot analysis of the lysates were carried out. QRT-PCR was carried out with TaqMan RT-PCR. RNA was purified from lymph node lysates using RNeasy Mini Kit (Qiagen), and then the purified RNA was subjected to TaqMan one-step RT-PCR universal master mix (ABI) according to the manufacturer's instructions. The sequences of the forward and reverse primers designed for human CK19 were 5′-CAGATCGAAGGCCTGAAGGA-3′ and 5′-CTTGGCCCCT-CAGCGTACT-3′, respectively. The sequence of the TaqMan probe, containing a fluorescent reporter dye (FAM) at the 5′ end and a fluorescent quencher dye (TAMRA) at the 3′ end, was 5′-FAM-GCCTACCTGAA-GAAGAACCATGAGGAGGAA-TAMRA-3′. The primers and TaqMan probe were obtained from Applied Biosystems (ABI). All QRT-PCR reactions were done in duplicate.

In the CK19 Western blot analysis, lysate (20 μL) was added to 10 μL of loading buffer containing 150 mmol/L Tris-HCl, 300 mmol/L DTT, 6% SDS, 0.3% bromophenol blue, and 30% glycerol. The solution was boiled and electrophoresed on a polyacrylamide gel in the presence of

Table 1. CK19 mRNA expression in 2^3 mm^3 of metastatic foci

Case	Histology	CK19 mRNA (copy/μL)
1	Ductal carcinoma	2.3×10^4
2	Ductal carcinoma	1.1×10^4
3	Ductal carcinoma	4.7×10^3
4	Ductal carcinoma	5.0×10^4
5	Ductal carcinoma	1.0×10^4
6	Lobular carcinoma	1.4×10^5
7	Ductal carcinoma	2.0×10^4
8	Ductal carcinoma	6.7×10^4
9	Ductal carcinoma	2.4×10^4
	Average	3.0×10^4

NOTE: CK19 mRNA expression in 2^3 mm^3 of metastatic foci was estimated on the basis of the examination of serial sections (Fig. 3B).

Table 2. Clinicopathologic characteristics of patients

	Number of patients
Stage	
0	5
I A/B	41
II A/B	49
III A/B/C	5
IV	1
Nodal status	
pN0	60
pN1	35
pN2	2
pN3	4
Histopathologic type	
Invasive ductal carcinoma	87
Neuroendocrine carcinoma	1
Matrix producing carcinoma	1
Mucinous carcinoma	2
Apocrine carcinoma	1
Invasive lobular carcinoma	4
Ductal carcinoma *in situ*	5

SDS (PAG Mini; Daiichi Pure Chemicals). After electrotransfer to Immobilon-FL polyvinylidene difluoride membranes (Millipore), the membrane was blocked with skim milk (BD Bioscience) for 1 h at room temperature. The primary antibody, anti-CK19 (A53-B/A2; Santa Cruz Biotechnology), was diluted 1:500 with TBS-Tween 20 (TBS-T) solution, and the membrane was incubated at 4°C overnight with anti-CK19 antibody. The membrane was then washed with TBS-T and incubated with a secondary antibody conjugated with horseradish peroxidase, which was diluted 1:2,000 with TBS-T. After washing the membrane twice with TBS-T, CK19-CK19 antibody complex was visualized using the ECL-Advance detection kit (GE Healthcare). The intensity of the signal in each band was evaluated by LumiAnalyst (Roche). CK19 protein concentration was determined based on a standard curve that was obtained by measuring known quantities of CK19 protein (Biodesign) of 0.15, 0.075, 0.038, and 0.018 ng/μL.

A cutoff value for CK19 protein expression between histopathologically positive and negative lymph nodes was determined by Western blot analysis of 37 histopathologically negative lymph nodes from 16 pN0 patients, 54 histopathologically negative lymph nodes from 17 pN1-3 patients, and 22 histopathologically positive lymph nodes from 12 patients (Figs. 3A and 5A). The cutoff value was determined by statistical analysis of the amount of CK19 measured by Western blot analysis of 37 histopathologically negative lymph nodes from 16 pN0 patients.

Results

Selection of the mRNA marker. We evaluated mRNAs for CK19, CEA, FOXA1, SPDEF, MUC1, and MGB1 using 11 histopathologically positive and 15 negative lymph nodes from 26 patients. The absolute mRNA expression levels of CEA and MGB1 in metastatic lymph nodes were not as high as expected, whereas the absolute expression levels of MUC1 mRNA in nonmetastatic lymph nodes was relatively high. For these reasons, CEA, MGB1, and MUC1 mRNAs were not selected for the OSNA assay.

The expression levels of CK19, FOXA1, and SPDEF mRNAs differed between histopathologically positive and negative lymph nodes. However, the lower limits of the expression levels of FOXA1 and SPDEF mRNAs in histopathologically positive lymph nodes were 4 to 30 times less than that of CK19 mRNA (Fig. 6). On the other hand, the detection limit of the OSNA assay was nearly equivalent to 32 threshold cycles of the RT-PCR system. An assay system should detect the upper limit of the expression levels of an mRNA marker in histopathologically negative lymph nodes. The upper limits of the threshold cycle of FOXA1 and SPDEF mRNAs were about 35 and 32,

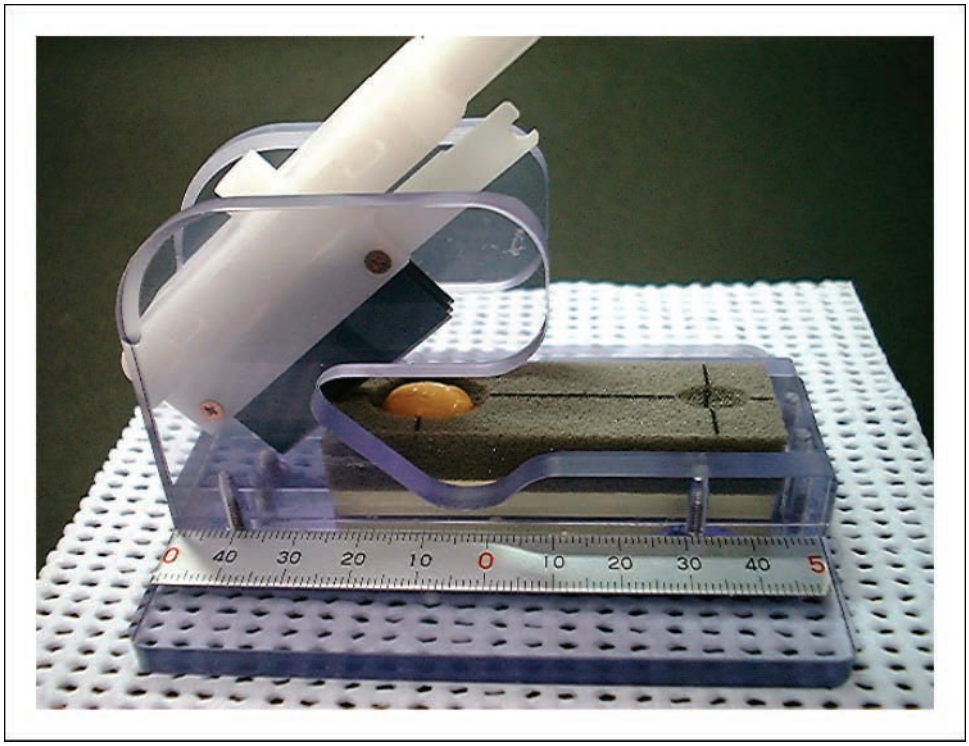

Fig. 4. Lymph node cutting device.

respectively. For these reasons, we determined CK19 mRNA to be the best marker for the OSNA assay.

OSNA assay. As shown in Fig. 1B, an inverse correlation between the threshold time in the RT-LAMP step and CK19 mRNA concentration was observed in a range of CK19 mRNA concentrations of 2.5×10^2 to 2.5×10^6 copies/μL, and both curves overlapped completely in the presence and absence of the lymph node lysate; the correlation coefficient value in both cases was 0.99. This result indicates that factors that may be present in lymph node lysates do not interfere with the OSNA assay.

Effect of lymph node size on the OSNA assay. The threshold time of the OSNA assay with 2.5×10^3 and 2.5×10^5 copies/μL of CK19 mRNA in a lysate obtained from 130 mg of lymph node was 10.9 and 9.6 min, respectively. The threshold time with 2.5×10^3 copies/μL of CK19 mRNA in a lysate obtained from a lymph node of 214, 354, and 428 mg was 10.7, 10.9, and 10.9 min, respectively, whereas the time with 2.5×10^5 copies/μL of CK19 mRNA in a lysate obtained from a lymph node of 214, 354, and 428 mg was 9.6, 9.7, and 9.7 min, respectively. The threshold times with 2.5×10^3 and 2.5×10^5 copies/μL of human CK19 mRNA in the lysates obtained from lymph nodes of 130, 214, 354, and 428 mg were within an acceptable error range. The results indicate that the OSNA assay is not influenced by lymph node size.

Amplification of genomic DNA by the OSNA assay. To exclude the possibility of genomic DNA amplification in the OSNA assay, we examined the OSNA assay using genomic DNA purified from lymph nodes. Genomic DNA was not amplified from either metastatic or nonmetastatic lymph nodes. The results indicate that the OSNA assay amplifies only CK19 mRNA.

Cutoff values. A cutoff value for the OSNA assay between histopathologically positive and negative lymph nodes was determined by the logarithmic normal distribution of CK19 mRNA copy numbers from 42 lymph nodes from pN0 patients. The average value of CK19 mRNA expression +3 SD was 2.5×10^2 copies/μL. Based on this analysis, we set the cutoff value at 2.5×10^2 copies/μL, which represents the upper limit of the copy numbers in the histopathologically negative lymph nodes from pN0 patients (Fig. 7A).

To validate the cutoff value, we examined CK19 mRNA expression in 42 histopathologically negative lymph nodes from 16 pN1-3 patients. Only one of these 42 cases showed $>2.5 \times 10^2$ copies/μL CK19 mRNA (Fig. 7B). This lymph node showed 3×10^3 copies/μL of CK19 mRNA. This suggested that micrometastatic foci in block a or c (Fig. 3A) of the lymph node were included in the sample. On the other hand, CK19 mRNA expression in all 24 pathologically positive lymph nodes from 10 patients exceeded the cutoff value (Fig. 7C).

To obtain a cutoff value for CK19 mRNA expression between macrometastasis with metastatic foci $>2^3$ mm^3 and micrometastasis, we compared CK19 mRNA expression in serial sections of a lymph node with an area of metastatic foci and roughly estimated macrometastasis to be $>5 \times 10^3$ copies/μL, which is the lowest value of CK19 mRNA expression found in metastatic foci of 2^3 mm^3 (Table 1).

Accordingly, for the OSNA assay, we defined macrometastasis (++) as $>5 \times 10^3$ copies/μL of CK19 mRNA, micrometastasis (+) as 2.5×10^2 to 5×10^3 copies/μL, and nonmetastasis (-) as $<2.5 \times 10^2$ copies/μL.

Clinical study. All OSNA assays were carried out during surgery and were completed within 30 min. H&E and CK19 immunohistochemistry were used in the histopathologic examination.

Isolated tumor cells (ITC) are widely used as one of indicators in a nomogram-aiding treatment decisions. In the American Society of Clinical Oncology guidelines (10), ITCs are described as having unknown clinical significance, and there are insufficient data to recommend appropriate treatment, including axillary lymph node dissection. For this reason, we viewed ITC as negative.

Table 3 shows the results of CK19 immunohistochemistry in all samples with the H&E results given in parenthesis. H&E-based histopathology failed to detect 1 of 40 cases of macrometastasis and 3 of 5 cases of micrometastasis. Overall, the sensitivity of H&E-based histopathology was 91.1% based on the results of CK19 immunohistochemistry–based histopathology. The sensitivities of the one- and two-level CK19

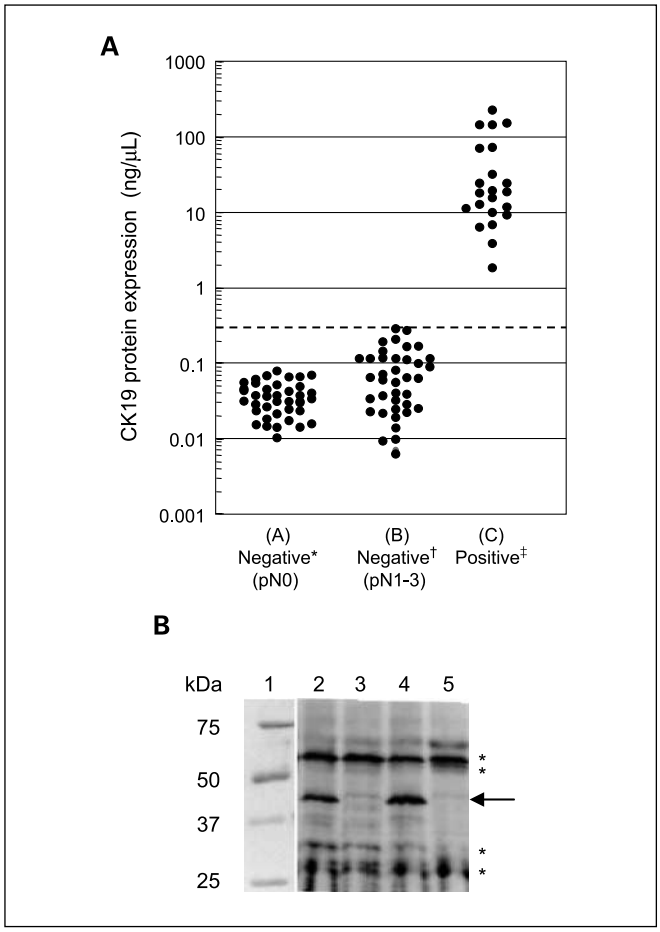

Fig. 5. CK19 protein expression in lymph node lysates. *A,* CK19 protein expression in histopathologically positive and negative lymph node lysates. *, histopathologically negative lymph nodes dissected from pN0 patients. †, histopathologically negative lymph nodes dissected from pN1-3 patients. ‡, histopathologically positive lymph nodes. The CK19 protein expression was determined by Western blot analysis (see Materials and Methods). Broken line, cutoff line between micrometastasis and nonmetastasis. The protein concentration of representative lymph node lysates used in this experiment was within the range of 8.7 to 11.6 μg/μL. *B,* a representative example of Western blot analysis of CK19 protein in lymph node lysates. Lane 1, molecular weight markers stained with Coomassie brilliant blue. Lanes 2 and 4, histopathologically positive lymph node lysate. Lanes 3 and 5, histopathologically negative lymph node lysate. Arrow, CK19 protein. *, nonspecific bands. The vertical scale shows molecular weights.

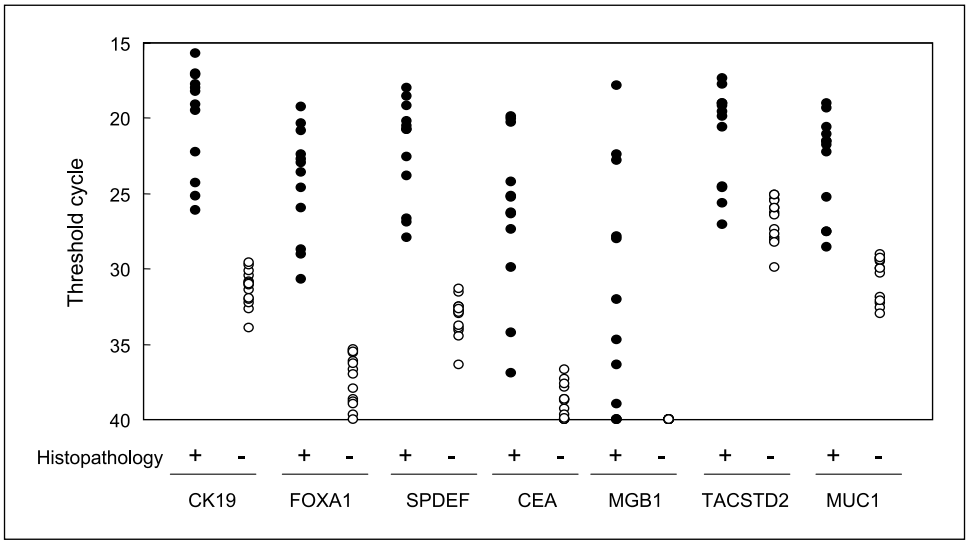

Fig. 6. Expression of mRNA markers in histopathologically positive and negative lymph nodes. The selected mRNA markers (CK19, FOXA1, SPDEF, CEA, MGB1, TACSTD2, and MUC1) were evaluated by QRT-PCR using 11 histopathologically positive (●) and 15 negative (○) lymph nodes from 26 patients.

immunohistochemistry–based histopathologies were 86.7% and 91.1%, respectively, based on the results of three-level CK19 immunohistochemistry–based histopathology (Supplementary Table S3).

The concordance rate between the OSNA assay and the CK19 immunohistochemistry–based three-level histopathology for 325 lymph nodes was 98.2%. The concordance rate for SLNs was 96.4%.

No false positive results were found with the OSNA assay of 144 histopathologically negative lymph nodes from 60 pN0 patients, in which neither micrometastasis nor macrometastasis was observed for serial sections from blocks b′ and d′ (Fig. 3C). Furthermore, the OSNA assay judged 13 ITC cases as negative. These results are summarized in Table 3.

Discordant cases. Six discordant cases were observed between the OSNA assay and CK19 immunohistochemistry–based histopathologic examination (Table 4). Four cases were micrometastasis according to the OSNA assay and were negative according to the CK19 immunohistochemistry–based histopathology. In any case, CK19 mRNA expression of $>10^3$ copies/μL was observed (Table 4). These four discordant cases came from pN1 and pN2 patients. In two of four cases, micrometastasis was observed in the multilevel examinations of blocks b′ and d′. On the other hand, two remaining cases (Table 4, *samples 5* and *6*) were negative according to the OSNA assay and micrometastasis according to the three-level histopathology. Samples 5 and 6 showed metastatic foci of 0.3 and 0.4 mm in the long axis, which were observed on surfaces i′ and ii′, respectively. When i′ and ii′ were histopathologically examined, about 0.2 mm was shaved from the surfaces of blocks b′ and d′. Therefore, the amount of metastatic foci in blocks a′ and c′ that were used for the OSNA assay (i.e., a′ and c′) could not be quantified.

We also measured the amount of CK19 protein by Western blot analysis of the lysate used in each discordance case. A cutoff value for CK19 protein expression between metastasis positive and negative lymph node was determined by the distribution of CK19 protein expression in 37 histopathologically negative lymph nodes from 16 pN0 patients. The distribution could be described as a logarithmic normal distribution. The statistical analysis indicated that an average value +3 SD was 0.13 ng/μL. Based on this analysis, the cutoff value was determined to be 0.3 ng/μL, which is the upper limit of the CK19 protein expression in 54 histopathologically negative lymph nodes from pN1-3 patients (Fig. 5A). Furthermore, CK19 protein expression in 22 histopathologically positive lymph nodes from 10 patients contained protein levels over the cutoff value.

Based on this cutoff value, we measured the amount of CK19 protein using quantitative Western blot analysis of the lysate for the OSNA assay of samples 1, 2, and 5. As described in Table 4, samples 1 and 2 showed an amount of CK19 protein expression equivalent to micrometastasis. Sample 5 exhibited no CK19 protein expression.

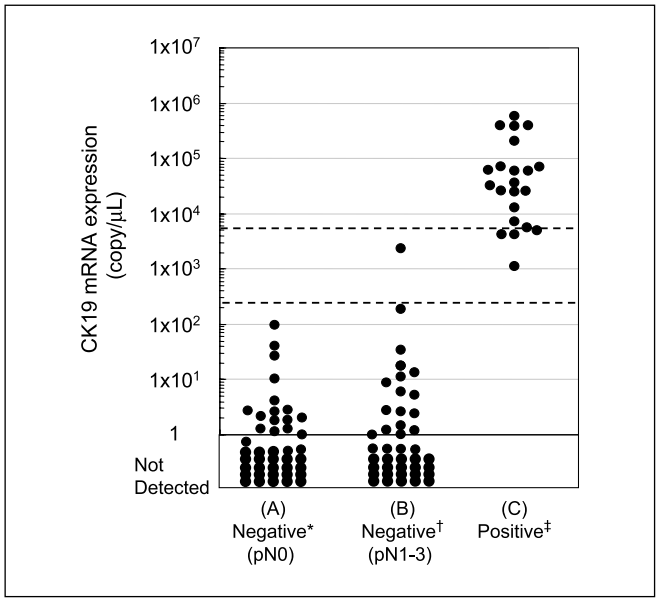

Fig. 7. CK19 mRNA expression in the OSNA assay carried out under the protocol A (Fig. 3 A). *, histopathologically negative lymph nodes dissected from pN0 patients. †, histopathologically negative lymph nodes dissected from pN1-3 patients. ‡, histopathologically positive lymph nodes. Top broken line, cutoff between macrometastasis and micrometastasis. Bottom broken line, cutoff between micrometastasis and nonmetastasis.

Table 3. Comparison of the OSNA assay with the histopathologic examination

Number of lymph nodes	OSNA*	Histopathologic examination †			
		Macrometastasis	Micrometastasis	ITC	Negative ‡
325 from 101 patients	++	34 (34)	0 (0)	0 (0)	0 (0)
	+	6 (5)	3 (1)	0 (0)	4 (0)
	-	0 (0)	2 (2)	13 (11)	263 (0)
81 SLNs from 49 patients	++	11 (11)	0 (0)	0 (0)	0 (0)
	+	1 (0)	2 (1)	0 (0)	1 (0)
	-	0 (0)	2 (2)	3 (2)	61 (0)
144 from 60 pN0 patients	++	0 (0)	0 (0)	0 (0)	0 (0)
	+	0 (0)	0 (0)	0 (0)	0 (0)
	-	0 (0)	0 (0)	3 (3)	141 (0)

*In the OSNA assay, (++), (+), and (-) show >5×10^3, 2.5×10^2 to 5×10^3, and <2.5×10^2 copies/μL of CK19 mRNA, respectively.
† Histopathologic examinations with H&E and CK19 immunohistochemistry were carried out in all samples. In cases where metastatic foci were observed in the histopathologic examination by either H&E or CK19 immunohistochemistry, the sample was categorized as macrometastasis, micrometastasis, or ITC. The results of the three-level CK19 immunohistochemistry–based histopathologic examination were determined by the consensus of three third-party pathologists. The number of lymph nodes judged to be positive based on the three-level H&E-based histopathologic examination is shown in parenthesis.
‡ No cancer cells were observed in either the immunohistochemistry- or H&E-based histopathologic examinations.

Discussion

The detection of lymph node metastasis by RT-PCR (37–40) and by QRT-PCR (12, 19–25) has been studied previously. CK19 mRNA has been described as having the highest sensitivity at nearly 90%. However, there are drawbacks using CK19 mRNA due to the concomitant amplification of pseudogenes in genomic DNA that lead to false positive results. For this reason, a combination of two or three markers has been used.

We evaluated 45 potential mRNAs and finally selected CK19 mRNA as the best marker for the OSNA assay. To use CK19 mRNA as a marker, we designed RT-LAMP primers that do not amplify the known CK19 pseudogenes (see Materials and Methods). In addition, the lymph node solubilization step in the OSNA assay was carried out at pH 3.5. At this pH, almost all genomic DNA precipitates out. Even when the sample still contained genomic DNA, DNA amplification is unlikely to occur in the OSNA assay because the RT-LAMP step is carried out at 65°C, a temperature at which genomic DNA typically does not denature. Indeed, purified genomic DNA from metastatic lymph nodes was not amplified in the OSNA assay.

In the present clinical study assessing 325 lymph nodes from 101 patients, an overall concordance rate between the OSNA assay and the CK19 immunohistochemistry–based three-level histopathology was 98.2%. A concordance rate of 96.4% was obtained with 81 SLNs from 49 patients. On the other hand, 1 of 40 macrometastatic cases and 2 of 5 micrometastatic lymph nodes, as defined by CK19 immunohistochemistry–based histopathology, were missed by H&E-based histopathology. Therefore, the sensitivity of three-level H&E-based histopathology was 93.3% based on the three-level CK19 immunohistochemistry–based histopathology. Furthermore, the sensitivity of one- and two-level CK19 immunohistochemistry–based histopathologies is 86.7% and 91.1%, respectively, based on the three-level CK19 immunohistochemistry–based histopathology (Supplementary Table S3). These results indicate that the performance of the OSNA assay is better than that of one- and two-level CK19 immunohistochemistry–based histopathologies and almost equivalent to three-level CK19 immunohistochemistry–based histopathology.

Chu and Wiess (41) reported that 98.2% of primary breast cancer tissues exhibit CK19 protein expression. Two of our authors (Tsujimoto and Tsuda) also examined the CK19 immunohistochemistry–based histopathologic examination of primary breast cancer tissues and found that there was no CK19 protein expression in 20 (2.2%) of 896 cases examined. However, low CK19 mRNA expression in lymph nodes has not been reported.

Table 4. Discordant cases between the OSNA assay and three-level histopathologic examination

Discordant case	CK19 mRNA (copy/μL)	CK19 protein (ng/μL)*	Histopathologic examination †	Nodal status
1	9.6×10^2	1.4	Negative	pN2
2	1.5×10^3	1.6	Negative	pN1
3	2.3×10^3	Not tested	Negative	pN1
4	3.6×10^3	Not tested	Negative	pN1
5	ND	0.04	Micrometastasis	pN1
6	ND	Not tested	Micrometastasis	pN1

Abbreviation: ND, not detected.
*Amount of CK19 protein was determined by Western blot analysis (see Materials and Methods).
† Results of CK19 immunohistochemistry–based histopathologic examination of the sections i′, ii′, and iii′ of protocol C (Fig. 3C).

In the present clinical study, CK19 immunohistochemistry–based histopathologic examination of two lymph nodes from one patient revealed metastatic foci smaller than macrometastasis despite the presence of macrometastasis defined by H&E-based histopathologic examination; the histologic type of this primary tumor was neuroendocrine carcinoma. These samples unequivocally had low CK19 expression. The OSNA assay of these samples was positive, indicating that CK19 mRNA was expressed despite the low protein expression found by CK19 immunohistochemistry.

In QRT-PCR studies in which several mRNA markers have been used (12, 19, 24, 25), the ability to quantitatively discriminate macrometastasis from micrometastasis has not been discussed. In the OSNA assay, the solubilization of a lymph node is followed by mRNA amplification. Regardless of the size of the lymph node, a constant portion of lysate is transferred to an RT-LAMP reaction. This indicates that the OSNA assay can, in principle, discriminate macrometastasis from micrometastasis and micrometastasis from nonmetastasis when the cutoff values of CK19 mRNA are properly set. To ensure the quantitative capacity of the OSNA assay, endogenous factors should not interfere with the RT-LAMP reaction. We showed that the presence of a lysate obtained from a lymph node (130-600 mg) did not interfere with the OSNA assay (Fig. 1B). A 600-mg sample of lymph node is equivalent to that having a diameter of about 1 cm. The presence of fat or the reagents that were used to identify SLNs, e.g., radioisotope colloid and blue dyes, did not also interfere with the reaction (data not shown).

We observed no false positive result in the OSNA assay from 144 histopathologically negative lymph nodes (60 pN0 patients). In the statistical analysis of the copy numbers of CK19 mRNA in these 144 lymph nodes, the average value of CK19 mRNA expression +3 SD was $<2.5 \times 10^2$ copies/μL, indicating that the probability of negative lymph nodes showing $>2.5 \times 10^2$ copies/μL is low in the OSNA assay. In the OSNA assay, all 13 ITC cases were judged as nonmetastasis (Table 3).

Based on the serial sectioning experiment (Table 1), the average copy numbers equivalent to 0.2^3, 0.3^3, and 0.4^3 mm^3 can be calculated to be 3.9×10^1, 1.3×10^2, and 3.1×10^2 copies/μL, respectively. Therefore, the cutoff value of 2.5×10^2 copies/μL in the OSNA assay can theoretically detect metastatic foci of 0.3^3 to 0.4^3 mm^3.

The OSNA assay identified 34 cases of macrometastasis out of 40 macrometastatic lymph nodes defined by the permanent three-level CK19 immunohistochemistry–based histopathology. The concordance rate was 85.0%. The remaining six cases were identified as micrometastasis. This is the first example of a molecular biological method with the potential to quantify the size of metastatic foci in a lymph node.

Six discordant cases were observed between the OSNA assay and CK19 immunohistochemistry–based histopathologic examination (Table 4). The quantitative Western blot analysis of the discordant cases (samples 1 and 2) clearly showed the presence of an amount of CK19 protein equivalent to micrometastasis. Although the possible presence of benign epithelial cells such as glandular inclusions in the lymph nodes cannot be eliminated, the results may be better explained by the presence of metastatic foci in the lymph nodes in light of the results of the specificity study and the amount of CK19 protein expression. Two other cases (Table 4, *samples 5* and *6*) were negative according to the OSNA assay, but were judged positive for micrometastasis according to three-level histopathology. These two cases showed metastatic foci of 0.3 and 0.4 mm. Therefore, the amount of metastatic foci in blocks a′ and c′ used for the OSNA assay cannot be estimated exactly. Indeed, in sample 5, the quantitative Western blot analysis of CK19 protein showed no expression of CK19 protein (Table 4).

The results of the clinical study indicate that using one-half of a lymph node in the OSNA assay gave nearly the same results as the three-level histopathology. It became clear in the clinical study conducted at six facilities that the OSNA assay is rapid enough to be done during surgery. Furthermore, the assay would be convenient and objective compared with the intraoperative immunohistochemistry-based histopathologic examination, which is usually done by an experienced pathologist (42, 43).

Acknowledgments

We thank Dr. T. Notomi (Eiken Chemical, Japan) for providing the CK19 cDNA, Dr. Masashi Takeda (National Hospital Organization Osaka National Hospital), Dr. Kenichi Wakasa (Osaka City University Medical School), and Dr. Tsuyoshi Okino (Osaka Sailor Hospital) for conducting the histopathology as third-party pathologists, and Dr. Satoshi Teramukai (Kyoto University) for managing the clinical information. We also thank the staff of the clinical and pathologic laboratories at each facility for their support. Thanks also go to Yoshihito Yamamoto, Yasumasa Akai, Katsuhito Matsumoto, Masahiro Nishida, Dr. Junyi Ding, Dr. Hideki Takata, and Kayo Hiyama for supporting the construction of the OSNA assay system. Finally, we express special thanks to Dr. Tameo Iwasaki, Sysmex Corporation, for his helpful advice and encouragement.

References

1. Donegan WL. Tumor-related prognostic factors for breast cancer. CA Cancer J Clin 1997;47:28–51.
2. van Diest PJ, Peterse HL, Borgstein PJ, Hoekstra O, Meijer CJ. Pathological investigation of sentinel lymph nodes. Eur J Nucl Med 1999;26:S43–9.
3. Weaver DL, Krag DN, Ashikaga T, Harlow SP, O'Connell M. Pathologic analysis of sentinel and nonsentinel lymph nodes in breast carcinoma: a multicenter study. Cancer 2000;88:1099–107.
4. Sabel MS, Zhang P, Barnwell JM, Winston JS, Hurd TC, Edge SB. Accuracy of sentinel node biopsy in predicting nodal status in patients with breast carcinoma. J Surg Oncol 2001;77:243–6.
5. Stitzenberg KB, Calvo BF, Iacocca MV, et al. Cytokeratin immunohistochemical validation of the sentinel node hypothesis in patients with breast cancer. Am J Clin Pathol 2002;117:729–37.
6. Luini A, Gatti G, Ballardini B, et al. Development of axillary surgery in breast cancer. Ann Oncol 2005;16:259–62.
7. Cote RJ, Peterson HF, Chaiwun B, et al. Role of immunohistochemical detection of lymph-node metastases in management of breast cancer. International Breast Cancer Study Group. Lancet 1999;354:896–900.
8. Van Diest PJ, Torrenga H, Borgstein PJ, et al. Reliability of intraoperative frozen section and imprint cytological investigation of sentinel lymph nodes in breast cancer. Histopathology 1999;35:14–8.
9. Torrenga H, Rahusen FD, Meijer S, Borgstein PJ, van Diest PJ. Sentinel node investigation in breast cancer: detailed analysis of the yield from step sectioning and immunohistochemistry. J Clin Pathol 2001;54:550–2.
10. Lyman GH, Giuliano AE, Somerfield MR, et al. American Society of Clinical Oncology guideline recommendations for sentinel lymph node biopsy in early-stage breast cancer. J Clin Oncol 2005;23:7703–20.
11. Tanis PJ, Boom RP, Koops HS, et al. Frozen section investigation of the sentinel node in malignant melanoma and breast cancer. Ann Surg Oncol 2001;8:222–6.
12. Hughes SJ, Xi L, Raja S, et al. A rapid, fully automated, molecular-based assay accurately analyzes sentinel lymph nodes for the presence of metastatic breast cancer. Ann Surg 2006;243:389–98.
13. Leidenius MH, Krogerus LA, Toivonen TS, Von Smitten KJ. The feasibility of intraoperative diagnosis of sentinel lymph node metastases in breast cancer. J Surg Oncol 2003;84:68–73.
14. Fortunato L, Amini M, Frrina M, et al. Intraoperative

examination of sentinel nodes in breast cancer: is the lass half full or half empty? Ann Surg Oncol 2004;11: 1005–10.

15. Pugliese MS, Kohr JR, Allison KH, Wang NP, Tickman RJ, Beatty JD. Accuracy of intraoperative imprint cytology of sentinel lymph nodes in breast cancer. Am J Surg 2006;192:516–9.

16. Caemon M, Olsha O, Rivkin L, Spira RM, Golomb E. Intraoperative palpation for clinically suspicious axillary sentinel lymph nodes reduces the false-negative rate of sentinel lymph node biopsy in breast cancer. Breast J 2006;12:199–201.

17. Salem AA, Douglas-Jones AG, Sweetland HM, Mansel RE. Intraoperative evaluation of axillary sentinel lymph nodes using touch imprint cytology and immunohistochemistry. Part II. Results. Eur J Surg Oncol 2006;32:484–7.

18. Brogi E, Torres-Matundan E, Tan LK, Cody HS III. The results of frozen section, touch preparation, and cytological smear are comparable for intraoperative examination of sentinel lymph nodes: a study in 123 breast cancer patients. Ann Surg Oncol 2005;12:173–80.

19. Mitas M, Mikhitarian K, Walters C, et al. Quantitative real-time RT-PCR detection of breast cancer micrometastasis using a multigene marker panel. Int J Cancer 2001;93:162–71.

20. Inokuchi M, Ninomiya I, Tsugawa K, Terada I, Miwa K. Quantitative evaluation of metastases in axillary lymph nodes of breast cancer. Br J Cancer 2003;89: 1750–6.

21. Weigelt B, Bosma AJ, Hart AA, Rodenhuis S, van 't Veer LJ. Marker genes for circulating tumour cells predict survival in metastasized breast cancer patients. Br J Cancer 2003;88:1091–4.

22. Weigelt B, Verduijn P, Bosma AJ, Rutgers EJ, Peterse HL, van't Veer LJ. Detection of metastases in sentinel lymph nodes of breast cancer patients by multiple mRNA markers. Br J Cancer 2004;90:1531–7.

23. Sakaguchi M, Virmani A, Dudak MW, et al. Clinical relevance of reverse transcriptase-polymerase chain reaction for the detection of axillary lymph node metastases in breast cancer. Ann Surg Oncol 2003;10: 117–25.

24. Backus J, Laughlin T, Wang Y, et al. Identification and characterization of optimal gene expression markers for detection of breast cancer metastasis. J Mol Diagn 2005;7:327–36.

25. Nissan A, Jager D, Roystacher M, et al. Multimarker RT-PCR assay for the detection of minimal residual disease in sentinel lymph nodes of breast cancer patients. Br J Cancer 2006;94:681–5.

26. Notomi T, Okayama H, Masubuchi H, et al. Loop-mediated isothermal amplification of DNA. Nucleic Acids Res 2000;28:E63.

27. Nagamine K, Hase T, Notomi T. Accelerated reaction by loop-mediated isothermal amplification using loop primers. Mol Cell Probes 2002;16:223–9.

28. Parida M, Posadas G, Inoue S, Hasebe F, Morita K. Real-time reverse transcription loop-mediated isothermal amplification for rapid detection of West Nile virus. J Clin Microbiol 2004;42:257–63.

29. Yoshikawa T, Ihira M, Akimoto S, et al. Detection of human herpesvirus 7 DNA by loop-mediated isothermal amplification. J Clin Microbiol 2004;42:1348–52.

30. Hong TC, Mai QL, Cuong DV, et al. Development and evaluation of a novel loop-mediated isothermal amplification method for rapid detection of severe acute respiratory syndrome coronavirus. J Clin Microbiol 2004;42:1956–61.

31. Poon LL, Leung CS, Tashiro M, et al. Rapid detection of the severe acute respiratory syndrome (SARS) coronavirus by a loop-mediated isothermal amplification assay. Clin Chem 2004;50:1050–2.

32. Fukuda S, Takao S, Kuwayama M, Shimazu Y, Miyazaki K. Rapid detection of norovirus from fecal specimens by real-time reverse transcription-loop–mediated isothermal amplification assay. J Clin Microbiol 2006;44:1376–81.

33. Schmitt AO, Specht T, Beckmann G, et al. Exhaustive mining of EST libraries for genes differentially expressed in normal and tumour tissues. Nucleic Acids Res 1999;27:4251–60.

34. Mori Y, Nagamine K, Tomita N, et al. Detection of loop-mediated isothermal amplification reaction by turbidity derived from magnesium pyrophosphate formation. Biochem Biophys Res Commun 2001; 289:150–4.

35. Mori Y, Kitao M, Tomita N, et al. Real-time turbidimetry of LAMP reaction for quantifying template DNA. J Biochem Biophys Methods 2004; 59:145–57.

36. Gusterson BA. The new TNM classification and micrometastases. Breast 2003;12:387–90.

37. Min CJ, Tafra L, Verbanac KM. Identification of superior markers for polymerase chain reaction detection of breast cancer metastases in sentinel lymph nodes. Cancer Res 1998;58:4581–4.

38. Manzotti M, Dell'Orto P, Maisonneuve P, Zurrida S, Mazzarol G, Viale G. Reverse transcription-polymerase chain reaction assay for multiple mRNA markers in the detection of breast cancer metastases in sentinel lymph nodes. Int J Cancer 2001;95: 307–12.

39. Noguchi S, Aihara T, Nakamori S, et al. The detection of breast carcinoma micrometastases in axillary lymph nodes by means of reverse transcriptase-polymerase chain reaction. Cancer 1994;74: 1595–600.

40. Bostick PJ, Huynh KT, Sarantou T, et al. Detection of metastases in sentinel lymph nodes of breast cancer patients by multiple-marker RT-PCR. Int J Cancer 1998;79:645–51.

41. Chu PG, Wiess LM. Keratin expression in human tissues and neoplasms. Histopathology 2002;40: 403–39.

42. Lee IK, Lee HD, Jeong J, et al. Intraoperative examination of sentinel lymph nodes by immunohistochemical staining in patients with breast cancer. Eur J Surg Oncol 2006;32:405–9.

43. Nahrig JM, Richter T, Kuhn W, et al. Intraoperative examination of sentinel lymph nodes by ultrarapid immunohistochemistry. Breast J 2003;9: 277–81.